Effect of Carbon Nanotubes Percentage on the Gage Factor in Structural Health Monitoring Sensors

N Youssef [1*], T Wafy[2], O Abdelsalam[2], O Dawood[3], Nariman E. Elbaly[3]

[1] Science and Technology Center of Excellence (STCE), Cairo
[2] Military Technical College, Egypt
[3] Mechanical Eng. Dept., Faculty of Engineering, University of Helwan, Cairo, Egypt.

*E-mail: nihal_yosef@yahoo.com

Abstract. Within the realm of composite health monitoring, carbon nanotubes have gained prominence as a crucial research subject, acclaimed for their superior performance and mechanical qualities. However, there has been inadequate emphasis on the capacity of carbon nanotube film sensors to monitor strain across different directions proficiently. A strain sensor has been developed for applications in structural health monitoring (SHM), using a carbon nanotube polymer material that enhances the interfacial bonding among the nanotubes. High-sensitivity polyurethane/multi-walled carbon nanotube (MWCNT) composite strain sensors were developed. This process unfolded in two stages: the initial stage concentrated on formulating a compound that detects strain by modifying the proportions of carbon nanotubes until effective strain sensing was realized. Nanocomposite films were created by adjusting MWCNT concentrations (0.75–2 wt %) using a direct mixing approach. The subsequent stage involved evaluating these nanocomposites' microscopic structure, thermal stability, and establishing a gauge factor at various strain levels. Generally, experimental findings indicate that the nanocomposite with 0.75 wt% MWCNT exhibited the most favorable strain sensing characteristics, achieving a gauge factor of 27.55 at 20% strain.

1. Introduction

Because of their exceptional mechanical, electrical, and thermal properties, polymer composites enhanced with carbon-based micro- and nanoscale materials are the topic of thorough investigation. Nanocomposites, in particular, offer customizable features, making them perfect for a variety of uses for a wide range of applications, and are simple to produce. [1]. Flexible and wearable strain sensors have garnered significant attention due to their growing demand for human motion monitoring, human-machine interaction, soft electronic skin, smart home appliances, soft robots, and structural health monitoring (SHM) [2, 3].

Recently, advanced systems like morphing aircraft, inflated spacecraft, and aerostats often experience significant (>10%) structural deformations, making it challenging to detect damage or cracks. Structural Health Monitoring (SHM) for aerospace applications offers a practical solution for continuously monitoring aircraft structures or security components. This approach enhances structures in critical areas, revolutionizes maintenance schedules, minimizes downtime, and boosts reliability and safety. Furthermore, incorporating an SHM system during the design phase improves aircraft performance, lowers fuel consumption, and allows for reduced aircraft weight and operating expenses [4, 5].

Resistive strain sensors require flexible conductive polymer composites (CPC) to be produced at low cost and high sensitivity. Rigid sensors, in contrast, have the ability to create wearable devices that are less comfortable, heavier, and less mobile [6, 7, 8]. As is well-known, conventional strain sensors are usually made from metals and semiconductors, which are rigid, have limited stretchability (less than 5%), and have low gauge factor (GF=2:5). They find it difficult to satisfy the requirements of wearable strain sensors as a result [9].

Strain sensors based on pure carbon nanomaterial films exhibit superior piezoresistive sensitivity, approximately 2 to 10 times higher than metal-foil strain gauges, especially at microstrains. However, they have limitations in handling large strains due to their low elongation at break. Conductive polymer nanocomposites incorporating carbon nanofillers offer a promising solution for strain sensors in SHM applications due to their excellent flexibility and capacity to maintain or recover electrical conductivity [10, 11].

Nanomaterials like carbon black (CB), carbon nanotubes (CNTs), graphene, metal nanowires, and metal nanoparticles are being investigated by numerous research groups, as sensitive materials for flexible strain sensors. CNTs are particularly appealing for flexible strain sensors in CPCs due to their outstanding mechanical strength, electrical conductivity, and high aspect ratio [12]. These sensors are typically made by combining these nanomaterials with soft polymers to produce stretchable support materials. Thermoplastic polymers like polymethyl methacrylate, polystyrene (PS), polyurethanes (PU), rubber such as polydimethylsiloxane (PDMS), and thermosetting polymers like epoxy resins are some of the most well-known polymers used to make CNT/polymer composite strain sensors [13].

Adding CNTs to polymers greatly enhances their electromechanical properties, increasing their Young's modulus and tensile strength, thereby improving their sensing performance. These sensors are frequently made using mixing techniques (such as melt-mixing, solution-mixing, and chemical synthesis techniques). Mixing methods entail uniformly blending the polymers and nanomaterials to create nanocomposite structures; these techniques are straightforward and scalable, but they necessitate to high dispersion of filler in the matrix [14].

The conductive network's evolution primarily determines the strain-sensing performance of the CPC during the stretching and releasing process. The distribution status, aspect ratio, and dimensionality of the conductive fillers, in addition to the matrix's physical and chemical characteristics, can all have an impact on this evolution [15]. The successful implementation of these functionalities relies heavily on the choice of filler-matrix combination and the composite manufacturing process. [16].

Earlier studies explored the impact of MWCNT filler on the strain-sensing capabilities of CPCs. Slobodian et al. [17]conducted a study using a polyurethane/carbon nanotube composite as a strain sensor. They evaluated the sensor's performance at different strain levels and found that at 8.7% strain, the gauge factor was 46. The sensor retained its conductivity even after being elongated up to approximately 300% strain. At near-breaking point strain, a gauge factor of 450 was achieved. Furthermore, the sensor demonstrated resilience under over 1,000 sine wave deformation cycles at around 6.5% strain. Kumar et al. [18] discussed the development of nanocomposites made from thermoplastic polyurethane (TPU) and multi-walled carbon nanotubes (MWCNTs) for strain-sensing applications at different MWCNT concentrations. They found that gauge factors (GF) varied by MWCNT concentration at low strain levels: for instance, 0.3 wt% MWCNT provided a GF of 22 at 15% strain, while higher strains saw much larger GF values up to 7935 at 185% strain for 1.0 wt% MWCNT.

In this work, a cost-effective and environmentally friendly technique for producing highly sensitive strain sensors using PU as the polymer matrix and different weight percentages of

(MWCNT) as a conductive carbon nano-filler (ranging from 0.75 to 2 wt%). The microstructure of the resulting nanocomposites was analyzed using SEM microscopy. Thermal properties of the composites with different CNT contents were examined through thermogravimetric Analysis (TGA). Additionally, sensor reliability was assessed by monitoring changes in electrical resistance using a four-point probe (4PP) under different mechanical strains.

2. Experiments

2.1 Materials

Multi-Wall Carbon Nanotubes (MWCNTs) were sourced from the Egyptian Petroleum Research Institute (EPRI), with an average diameter of 25 nm and length of up to 5 μm (aspect ratio =100), and purity>90%. The two components (A and B) of polyurethane (PU) and pro-solve PU were purchased from Prokem Special Chemicals.

2.2 Sample preparation

Nanocomposite thin films containing different weight percentages of MWCNTs (0.75%, 1%, 1.5%, and 2%) were synthesized through a direct mixing technique according to the procedure illustrated in Figure 1. The dispersion was achieved through a direct mixing technique, recognized for its simplicity and efficiency. Firstly, MWCNTs were weighted to achieve weight percentages (Figure 1a), then mixed into pre-solved polyurethane (PU) to ensure compatibility and reduce viscosity (Figure 1b). This mixture underwent a sonication process using a water bath sonicator at a temperature of 25˚C and an ultrasonic power of 140 W for 30 minutes to enhance CNT distribution, as shown in (Figure 1c).

PU resin was incorporated into the sonicated mixture (Figure 1d) and further sonication for 2 hours enhanced CNT dispersion and minimized aggregation (Figure 1e). The mixture was magnetically stirred for 2 hours to ensure a uniform distribution of CNTs. Then the solvent was evaporated (Figure 1f). This continuous stirring helps achieve uniform dispersion of CNTs in the polyurethane (PU) matrix and aids in solvent evaporation to prevent settling particles or agglomeration that could degrade the film quality. In the next step, component B of PU is added to initiate the curing process of the PU. This component triggers the cross-linking reaction, resulting in the formation of a robust polymer network. The curing agent should be thoroughly mixed into the dispersion for 15 minutes to ensure uniform distribution (Figure 1g).

The glass substrates are cleaned with acetone to eliminate impurities and residues that could affect adhesion and film quality, then the prepared mixture is applied to a substrate using a screen printing method, which offers precise control over film thickness and coverage, making it ideal for creating uniform layers (Figure 1h). Following deposition, the films are protected with an isolation foil to regulate thickness during curing and ensure even film formation, the sample thickness was adjusted to be 400 μm (Figure 1i).

After curing, the films are cut to the specified dimensions of 2.5 cm ×1 cm to meet experimental requirements. For crisp edges and well-defined shapes, cutting should be done with precision tools. Figure 2 illustrates a picture of PU/CNTs nanocomposite thin film with different weight percentages.

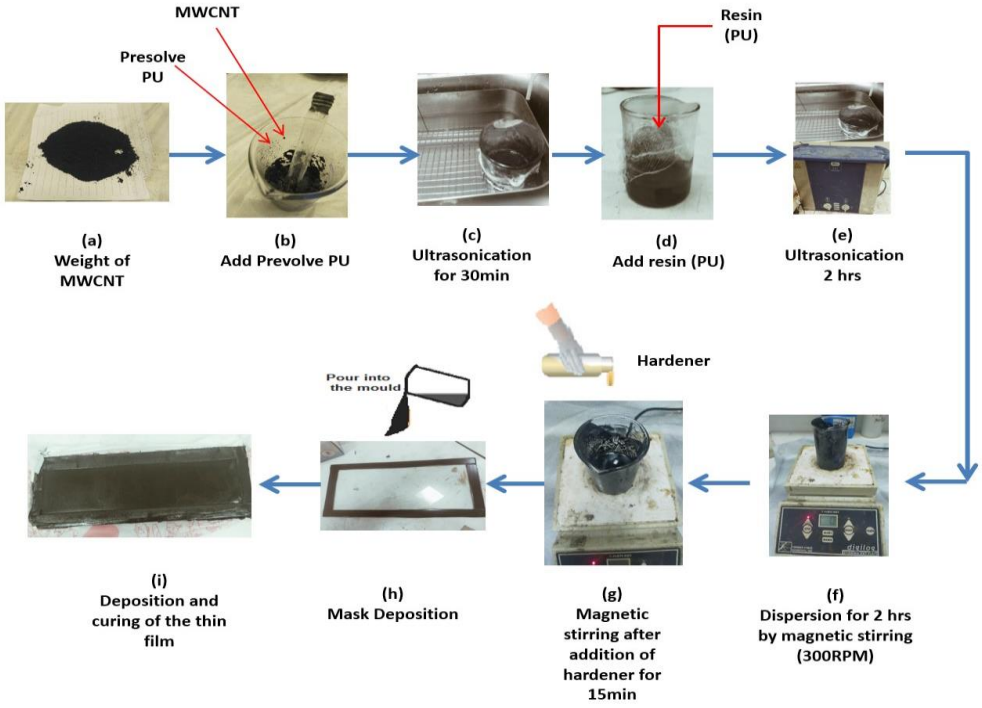

Figure 1. Step-by-step schematic of the PU/MWCNT nanocomposite thin film fabrication process.

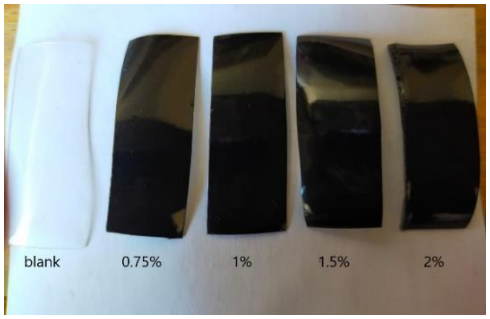

Figure 2. Image of PU/CNT nanocomposite thin films with varying CNT weight percentages.

2.3 Samples Characterization

The nano-composite film's microscopic structure of the PU/CNT (polyurethane/Carbon Nanotubes) was analyzed using field emission scanning electron microscopy (FESEM). Micrographs were taken of the fractured surface obtained from the tensile test. The samples were coated with a thin layer of gold using a vacuum evaporator to enhance image clarity. The samples' surface morphology and structural characteristics were further examined with high-resolution scanning electron microscopy (SEM) using an FEI Quanta FEG 250 instrument.

Thermo-gravimetric analysis (TGA) was utilized to study the thermal stability of polyurethane/CNT nanocomposites and their samples. This technique is used to measure mass changes, thermal decomposition, and thermal stability of various composite materials, including polymers, and helps establish their applicable temperature ranges. The TGA measurements were performed using a PerkinElmer instrument (USA) over a temperature range of 30–600°C, under a

nitrogen flow rate of 20 mL/min, and a heating rate of 10°C/min. The analysis provided the residual weight percentage of the composites at 600°C.

Monitoring resistance changes under strain is crucial for developing strain sensors and other applications in materials science. The four-point probe (FPP) method, an industry standard, is commonly used to accurately measure sheet resistance by eliminating contact resistance. A complete FPP measuring system consists of a mechanical unit with a probe assembly, an electronic module with a constant-current source/sink, and a voltmeter. Four equally spaced electrodes are used to contact the specimen under test, as shown in Figure 3. The FPP utilizes an ADC to convert analog voltage and/or current signals into digital signals (A to D converter). These digital signals are then used to determine and display the final measurement values. This digital conversion process is essential for achieving the high accuracy and consistency required for semiconductor measurements. The current source/sink applies a constant current through the specimen, while the voltmeter measures the voltage developed in the sample. The ratio of the measured voltage (V) to the constant current (I) gives the resistance (R) of the sheet [19].

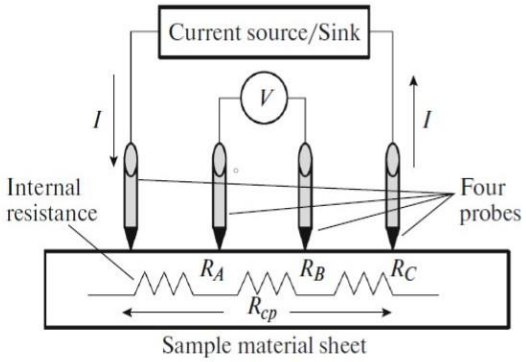

Figure 3. Scheme for a Four-point probe system [19].

The electromechanical behavior of a material is crucial for its effectiveness as a strain sensor. Changes in electrical resistance were measured in ohms per square (Ω/sq) for thin film material, regardless of its size, using a Semi Lab FPP-1000 four-point probe at room temperature. Data was collected via the Sam Suite V1.2.54.0 software, the software associated with a four-point probe (FPP) system plays a crucial role in data acquisition analysis. Axial longitudinal strains were applied to the samples, starting from an initial length of 25 mm (0% strain) as shown in Figure 4 and increasing to 30 mm (20% strain) in 4% increments. The sensors exhibited significant changes in electrical resistance under tensile stress, primarily due to developing a conductive network. The four-point probe (FPP) was utilized for this study, as shown in Figure 5. The gauge factor (GF) of a strain sensor is typically determined by the slope of the curve showing the relative change in electrical resistance ($\Delta R/R0$) in response to strain, which is calculated as $\Delta R/(R0\ \varepsilon)$, where ΔR is the resistance change, R0 is the initial resistance, and ε is the applied strain.

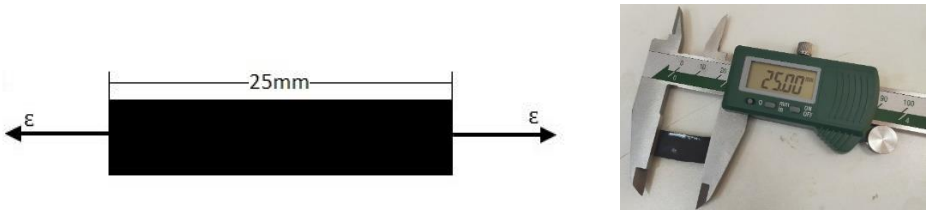

Figure 4. The strain sensors under axial tensile strain

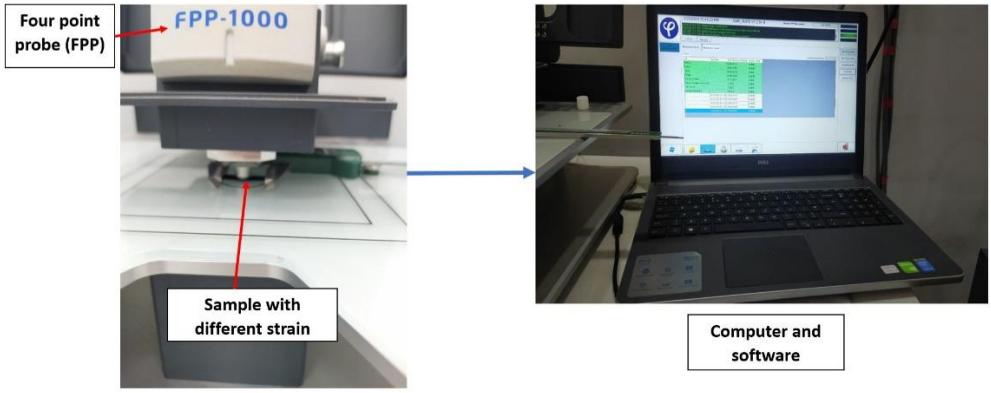

Figure 5. Setup for measuring resistance changes under different strain conditions.

3. Results and Discussion

3.1. Characterization of the PU Composites by SEM

The dispersion of CNT notably determines the performance of PU/CNT composites within the matrix material. The analysis of the Field Emission Scanning Electron Microscopy (FESEM) emphasizes the importance of CNT dispersion in polyurethane (PU) composites for strain sensor applications.

The images obtained contribute to a better understanding of the morphology, distribution, and uniformity of CNT in the polymer composite. The images of Scanning Electron Microscopy (FESEM) in Figures 6A-6F focus on the fractured surface which results from a tensile test and are coated with a thin layer of gold to enhance the resolution of the images. SEM images in Figure 6(A) display the smooth and uniform surface of the unmodified PU matrix, which indicates its homogeneity before the introduction of CNT. This establishes a stable base for integrating conductive fillers such as CNT. The CNT particles, as depicted in Figure 6(B), reveal a dense, interconnected network of CNTs, Individual CNTs are visible, and their tubular nature is obvious. The nanotubes are entangled, forming a web-like structure typical for CNTs due to their high aspect ratio and flexibility. The tightly packed network of CNTs may hinder their dispersion in a matrix, reducing their effectiveness in enhancing properties

Figures 6(C), 6(D), 6(E), and 6(F) illustrate composites with different CNT concentrations. At 0.75,1 wt% (Figure 5-C and 5-D), the dispersed CNT particles form good conductive networks, the nanotubes are more evenly distributed in the matrix, with fewer noticeable clusters or agglomerations are visible, indicating good interaction between CNTs and the matrix. When the CNT concentration increases to 1.5 wt% (Figure 6-E) the dispersion of CNTs appears relatively poor, as the CNTs seem to be primarily concentrated in localized regions rather than being uniformly distributed throughout the matrix. At 2 wt% (Figure 6-F), the dispersion of CNTs appears to be highly irregular and dominated by agglomerations. The image shows that CNTs form large clusters or are embedded in dense regions without adequate separation within the matrix. This indicates poor dispersion, likely caused by ineffective processing or insufficient interaction between the CNTs and the matrix.

The SEM analysis highlights the importance of achieving an optimal CNT concentration (0.75–1 wt%) to balance dispersion, network formation, and overall performance in PU/CNT composites. Excessive CNT loading can result in clustering, diminishing the benefits of their incorporation and compromising the composite's effectiveness for advanced applications

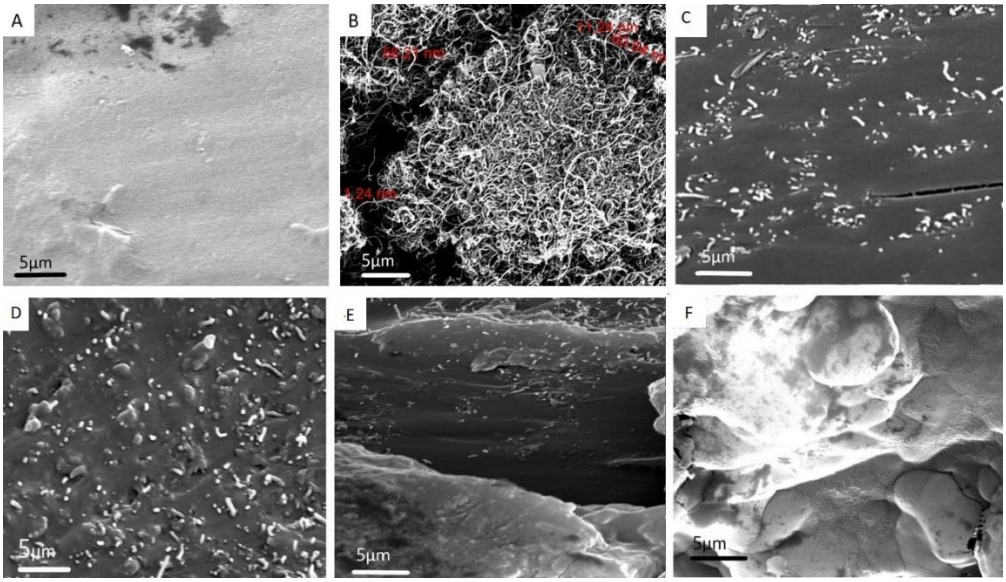

Figure 6. Surface morphologies of PU/CNT composites with different CNT contents: (A) neat PU, (B) MWCNT, (C) 0.75% CNT, (D) 1% CNT, (E) 1.5% CNT, and (F) 2% CNT, shown at a scale bar of 5µm.

3.2 Thermal stability of PU /CNT

All the gravimetric measurements of pure PU and its nanocomposites with CNT are shown in Figure 7. The thermal behavior of polyurethane at different Carbon Nanotubes (CNT) concentrations is analyzed, showing distinct stages of weight loss with increasing temperatures. The first stage, occurring below 100°C, involves slight weight loss due to the evaporation of absorbed water. Between temperatures of 100°C and 300°C, weight reduction results from the removal of oxygen-containing surface compounds. Up to around 200°C, the material exhibits minimal weight loss, indicating good thermal stability at lower temperatures. The second stage (300°C-500°C) is characterized by rapid weight loss as the polyurethane matrix decomposes and volatile components are released. In the final stage (500°C-600°C), most of the material breaks down, leaving minimal residue, demonstrating high thermal stability. Residual material at these temperatures remains stable.

The addition of CNT influences thermal stability by altering the degradation profile. CNT enhances the material's resistance to thermal decomposition at lower temperatures and modifies the decomposition process at higher temperatures. This improvement in thermal stability makes the composite suitable for applications in high-temperature environments, such as industrial machinery, automotive parts, and wearable electronics that are exposed to body heat or moderate heat during operation.

The graph illustrates a decrease in weight percentage with increasing temperature, suggesting material degradation, higher CNT content (from 0.75% to 2%) enhances thermal stability, the sample with 2% CNT exhibits the greatest resistance to thermal degradation, and towards the end of the test (~600°C), samples with higher CNT content show better weight retention, indicating enhanced formation facilitated by CNT acting as a thermal barrier. The results suggest that incorporating CNT enhances the thermal properties of polyurethane by delaying decomposition and increasing residue formation.

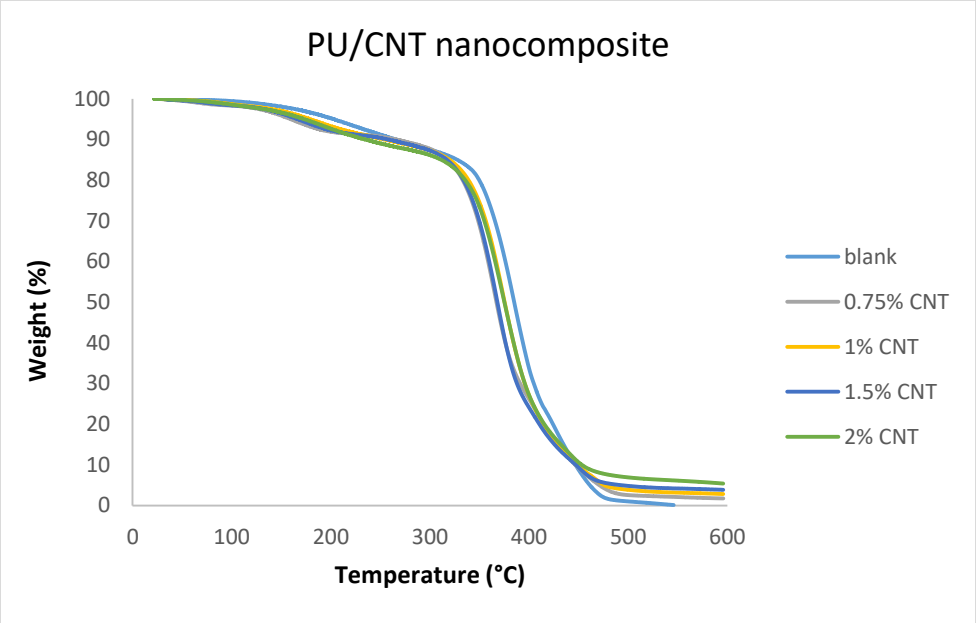

Figure 7. TGA analysis of PU and its composites with different CNT contents.

3.3 Piezoresistive response of MWCNTs/PU composite films

Figure 8 highlights the relationship between resistance change ($\Delta R/R_0$) and the initial resistance R_0 when the nanocomposite PU/CNT is exposed to strains in the range of 4% to 20%. The film's resistance increases under tensile strain due to microstructural changes, such as the stretching or breakage of conductive pathways within the composite. This increase in resistance occurs when the distance between CNT particles increases under stress and disrupts conductivity. Factors like tunneling, variations in contact resistance between carbon nanostructures, and the reformation or breaking of conductive networks contribute to this effect. The 0.75% CNT composition shows the greatest strain sensitivity, with a steeper response curve, indicating higher responsiveness at lower CNT concentrations. In contrast, higher CNT content reduces strain sensitivity, as seen in the slopes of the curves. This reduced sensitivity may result from denser conductive pathways and particle agglomeration, which can cause irregularities in the network and inconsistent electrical signals under strain, thereby lowering the overall response of the material.

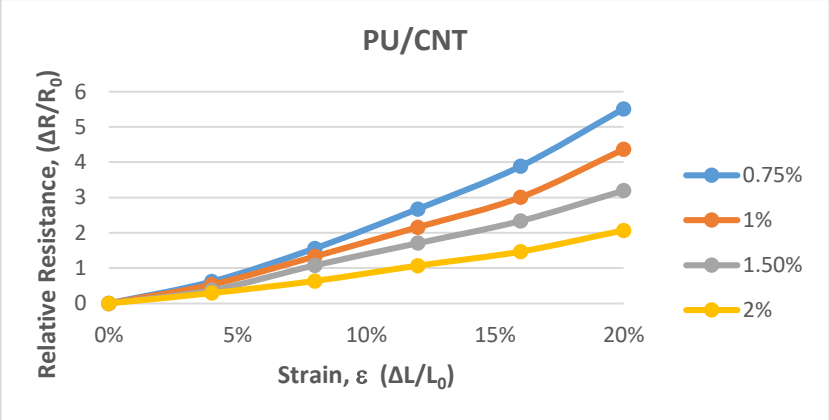

Figure 8. Piezoresistive behavior of PU/CNT nanocomposites.

The CNT content has a notable impact on the slope of the (ΔR/Ro) curve, with higher CNT concentrations leading to a lower slope. This slope, referred to as the strain gauge factor, measures the ratio of the relative resistance change (ΔR/Ro) to the applied strain (ε). A higher gauge factor reflects greater sensitivity of the material's resistance to deformation. In Table 1, the gauge factor is analyzed for polyurethane (PU) containing different CNT weight percentages (0.75% to 2%) under various strain levels (4% to 20%).

The gauge factor is expressed as:

$$GF = \frac{(R-R_0)/R_0}{(l-l_0)/l_0} = \frac{(\Delta R/R_0)}{\varepsilon} \quad (1)$$

Table 1. Gauge Factor (GF) Values at Different Strain Levels and Carbon Nanotube Percentages

Carbon Nanotube % (CNT%)	(GF) at 4% Strain	(GF) at 8% Strain	(GF) at 12% Strain	(GF) at 16% Strain	(GF) at 20% Strain
0.75%	15.44931	19.45876	22.26874	24.26881	27.5517
1.00%	13.26849	16.60421	17.9812	18.79127	21.81764
1.50%	9.300831	13.46082	14.20795	14.60913	15.97458
2.00%	7.269043	7.918817	8.885524	9.16129	10.33039

The gauge factor of PU/CNT films with different CNT concentrations (ranging from 0.75% to 2% wt) was assessed as a function of applied strain, as shown in Table 1. It is observed that the slope of the $\Delta R/R_0$ curve varies with the CNT content, with higher CNT concentrations resulting in a smaller slope. The slope of this curve represents the gauge factor of the strain sensor, where a larger slope indicates a higher gauge factor, meaning the composite film is more sensitive to strain. The gauge factor for the film with 0.75% CNT is 27.55, while for films with 1%, 1.5%, and 2% CNT, the values are 21.82, 15.97, and 10.33, respectively. At low concentrations of CNT, an increase in the gauge factor (GF) value is observed when axial longitudinal strains are applied to the samples. This increase occurs during the disconnection phase of CNTs. At higher concentrations, the formation of dense CNT networks in the PU matrix enhances its overall conductivity. In comparison, conventional foil strain sensors typically have a gauge factor of around 2.0, highlighting the significantly higher sensitivity of the composite films produced with this method.

The strain-resistance behavior of PU/CNT nanocomposites emphasizes the significant impact of CNT concentration on their response to mechanical deformation. The observed trends offer valuable insights into how the material's microstructure and electrical conductivity interact when subjected to strain.

The steep slope in the 0.75% CNT curve indicates significant changes in resistance under strain. This behavior can be attributed to the sparse distribution of CNTs in the matrix, which leads to increased disruption of conductive pathways when strain stretches the matrix. Additionally, a more pronounced tunneling effect occurs, where small changes in the distance between CNTs significantly impact conductivity. This composition shows potential for applications requiring high strain sensitivity. The strain sensitivity decreases as the CNT content increases (1%, 1.5%, 2%). This is attributed to a denser network of CNTs that maintains conductivity under strain by providing multiple redundant pathways. However, particle agglomeration may occur at higher CNT content, leading to non-uniformity in the conductive network and reduced responsiveness. Lower CNT concentrations are ideal for sensors that require high responsiveness. On the other hand, higher CNT

concentrations offer more stable and consistent electrical signals, making them better suited for applications such as structural monitoring or wearable electronics.

4. Conclusion

This study presents a scalable and cost-effective approach to fabricating flexible strain sensors based on CNT-reinforced polyurethane (PU) nanocomposites. Key findings reveal that uniform dispersion of CNT is achieved at low concentrations, while higher ones lead to agglomeration. Incorporating CNT enhances the thermal stability of PU, making the composites suitable for high-temperature applications. The electrical resistance of the films increases under tensile stress due to particle separation, at lower CNT concentrations (0.75% and 1%) resistance changes are larger and sensitivity is higher than at higher concentrations (1.5% and 2%). The strain-sensing performance, influenced by CNT distribution, is characterized by a high gauge factor ranging from 10.33 to 27.55 at lower CNT concentrations. On the other hand, the gauge factor decreases at all strain levels as the CNT percentage rises. These results open the door for developments in multipurpose materials by highlighting the potential of PU/CNT nanocomposites for application in flexible and wearable sensor technologies.

5. Reference

[1] S. Dul, A. Pegoretti and L. Fambri, "Fused Filament Fabrication of Piezoresistive Carbon Nanotubes Nanocomposites for Strain Monitoring," Frontiers in Materials, vol. 7, no. 12, pp. 1-13, 2020.

[2] L. Huang, J. Chen, Y. Xu, D. Hu, X. Cui and D. Shi, "Three-dimensional light-weight piezoresistive sensors based on conductive polyurethane sponges coated with hybrid CNT/CB nanoparticles," Applied Surface Science, vol. 548, pp. 149268- 149275, 2021.

[3] Z. X, X. D., Z. W, Z. Y and L. Y., "Flexible and high-performance piezoresistive sensors based on carbon nanoparticles @polyurethane sponges," Composites Science and Technology, pp. 108437- 108457, 2020.

[4] M. Q. Le, J.-F. Capsal, M. Lallart, Y. Hebrard, A. V. D. Ham, N. Reffe, L. Geynet and P.-J. Cottinet, "Review on energy harvesting for structural health monitoring in aero nautica lapplications," Progress in Aerospace Sciences, pp. 1-11, 2015.

[5] F. Yin, D. Ye, C. Zhu, L. Qiu and Y. Huang, "Stretchable, Highly Durable Ternary Nanocomposite Strain Sensor for Structural Health Monitoring of Flexible Aircraft," sensors, vol. 2677, pp. 1-12, 2017.

[6] Y. Gaoa, X. Fang, J. Tana, T. Lub, L. Pan and F. Xuan, "Highly Sensitive Strain Sensors Based on Fragmentized Carbon Nanotube/Polydimethylsiloxane Composites," Nanotechnology, vol. 200237, pp. 1-29, 2018.

[7] H. Souri, H. Banerjee, A. Jusufi, N. Radacsi, A. A. Stokes, I. Park, M. Sitti and M. Amjadi, "Wearable and Stretchable Strain Sensors: Materials, Sensing Mechanisms, and Applications," ADVANCED INTELIGENT SYSTEMS, vol. 2000039, pp. 1-27, 2020.

[8] A. Georgopoulou, S. Srisawadi, P. Wiroonpochit and F. Clemens, "Soft Wearable Piezoresistive Sensors Based on Natural Rubber Fabricated with a Customized Vat-Based Additive Manufacturing Process," Polymers, vol. 2410, pp. 1-14, 2023.

[9] Z. Zhuang, N. Cheng, L. Zhang, l. Liu, J. Zhao and H. Yu, "Wearable strain sensor based on highly conductive carbon nanotubes polyurethane composite fibers," Nanotechnology, pp. 1-24, 2020.

[10] G.-. J. Zhu, P.-g. Ren, H. Guo, Y.-L. Jin, D.-X. Yan and Z.-M. Li, "Highly Sensitive and Stretchable Polyurethane Fiber Strain Sensors with Embedded Silver Nanowires," Applied Materials & Interfaces, pp. 1-30, 2019.

[11] K. Ke, V. S. Bonab, D. Yuan and I. Manas-Zloczower, "Piezoresistive Thermoplastic Polyurethane Nanocomposites with Carbon Nanostructures," CARBON, vol. 37, pp. 1-24, 2018.

[12] D. Guo, X. Pan and H. He, "A simple and cost-effective method for improving the sensitivity of flexible strain sensors based on conductive polymer composites," Sensors and Actuators, vol. 298, p. 111608, 2019.

[13] L. Zhu, X. Zhou, Y. Liu and Q. Fu, "Highly Sensitive, Ultra-Stretchable Strain Sensors Prepared by Pumping Hybrid Fillers of Carbon Nanotubes /Cellulose Nanocrystal into Electrospun Polyurethane Membranes," ACS Applied Materials & Interfaces, pp. 1-36, 2019.

[14] Y. Zheng, Y. Li, K. Dai, M. Liu, K. Zhou, G. Zheng, C. Liu and C. Shen, "Conductive thermoplastic polyurethane composites with tunable piezoresistivity by modulating the filler dimensionality for flexible strain sensors," Composites: Part A, 2017.

[15] O. Sanchez-Sobrado, D. Rosario, R. Losada and E. Rodriguez, "Conductive Smart Nanocomposite Polymeric Materials for Structural Health Monitoring and Motion Detection," Research Square, vol. 1, no. DOI: https://doi.org/10.21203/rs.3.rs-2312829/v1, pp. 1-11, 2022.

[16] E. D. Meo, S. Agnelli, A. Veca, V. Brunella and M. Zanetti, "Piezoresistive and Mechanical Behavior of CNT Based Polyurethane Foam," Compos. Sci, vol. 4, pp. 131-145, 2020.

[17] P. Slobodian, R. Danova, R. Olejnik, J. Matyas and L. Münster, "Multifunctional flexible and stretchable polyurethane/carbon nanotube strain sensor for human breath monitoring," vol. 30, p. 1891–1898., 2019.

[18] S. Kumar, T. K. Gupta and K. M. Varadarajan, "Strong, stretchable and ultrasensitive MWCNT/TPU nanocomposites for piezoresistive strain sensing," Composites Part B, 2019.

[19] H. M. Fahad and A. Asif, "A Simple FPP Device for Pulsed Measurement of Sheet Resistance," INSTRUMENTS AND EXPERIMENTAL TECHNIQUES, vol. 64, p. 898–904, 2021.

Acknowledgment

All fabrication and (FPP) procedures were performed at Science and Technology Center of Excellence (STCE) at composite materials department. (TGA) analyses were performed in the main laboratories for chemical warfare, and (FESEM) of samples was employed in Desert Research Center.